

## Stability of ultrathin alumina layers on NiAl(110)

J. P. Pierce,\* N. C. Bartelt, R. Stumpf, and K. F. McCarty  
 Sandia National Laboratories, Livermore, California 94551, USA  
 (Received 20 January 2008; published 27 May 2008)

By observing with low-energy electron microscopy whether individual alumina islands grow or shrink for different substrate temperatures and  $O_2$  pressures, we determine the stability of thin oxide layers on the NiAl(110) surface. At each temperature, a well-defined  $O_2$  pressure exists where islands do not change in size. Yet we conclude that the oxide cannot be in thermodynamic equilibrium with  $O_2$  gas and NiAl bulk, because the  $O_2$  pressures needed to attain this state are 20 orders of magnitude higher than expected. We discuss what kinetic processes can lead to the observed steady state, where the  $O_2$  pressure needed for stability differs greatly from thermodynamic predictions.

DOI: [10.1103/PhysRevB.77.195438](https://doi.org/10.1103/PhysRevB.77.195438)

PACS number(s): 68.35.Md, 68.37.Nq, 68.60.Dv, 81.65.Mq

### I. INTRODUCTION

Determining whether phases at surfaces are at equilibrium, metastable, or unstable has long been recognized as important to understanding their synthesis and application.<sup>1</sup> If the surface phase is in equilibrium with the gas phase and the bulk of the substrate, thermodynamics governs the stability conditions. For example, Campbell recently considered the relative thermodynamic stability of compounds in their thin-film and bulk forms. He concluded that the material is more stable as a film that wets a surface than in bulk form.<sup>2</sup> That is, the equilibrium  $O_2$  pressure of a thin, wetting, oxide film should generally be lower than that of the bulk oxide. The thermodynamic data that determine equilibrium can be estimated from first-principle techniques<sup>3–6</sup> that consider the detailed atomic structure of the film and its interface with the substrate. A question needs to be considered when using such thermodynamic analysis to calculate the stability conditions of a particular system—is the thin surface phase in equilibrium with its environment, i.e., the substrate and the gas phase, under synthesis or application conditions?

Whether equilibrium is established can be seriously questioned. First, the combined substrate, thin-film, gas-phase environment may not be a closed system. For example, species may be leaving the surface, going either into the gas phase or substrate, without a balancing species flux to the surface. Second, the film and gaseous fluxes may have different temperatures, as is commonly the case for hot substrates in cold-walled vessels. Third, the rate of reaction between substrate and gas phase might be so slow that, at experimental time scales, no significant conversion of the substrate into its gas-phase-dictated equilibrium phase is observed.

In fact, the literature suggests that some film structures are often not in equilibrium with their environments. For example, Finnis *et al.*<sup>5</sup> noted that alumina on NiAl(100) and  $Ga_2O_3$  on CoGa(110) and (100) surfaces can be decomposed by vacuum annealing at much lower temperatures than anticipated from thermodynamic analysis. In addition, Lundgren *et al.*<sup>7</sup> found that there was a strong kinetic hindrance to forming the bulk form of PdO on Pd(100). In contrast, the measured stability of the surface oxide on Pd(111) agrees with thermodynamic predictions.<sup>8</sup>

Here, we determine the conditions under which ultrathin alumina films on NiAl(110) (Refs. 6 and 9) are stable in the

presence of gas-phase  $O_2$ . When NiAl(110) is exposed to small  $O_2$  doses at 800–1350 K, discrete structures of two different aluminum-oxide phases form on the surface.<sup>10,11</sup> One phase is the well-studied  $Al_{10}O_{13}$  phase,<sup>6,9</sup> whose complex structure is distinct from all bulk forms of alumina.<sup>6</sup> This surface oxide has two O layers, with an Al layer in between, and another Al layer next to the substrate. For simplicity, we refer to this phase as the “alumina islands.” The second oxide phase forms rods along the substrate’s [001] direction. We have previously characterized the morphology and growth kinetics of these rods, but not the stability of the rods and the islands.<sup>10</sup> Individual rods are several nanometers wide and can be several microns long. The rods are typically 1–4 atomic layers thick (0.2–0.8 nm). The rods are likely a variant of bulk alumina, although their structure and composition have not been determined.

We find that oxide islands grow (shrink) for  $O_2$  pressures above (below) unique values,  $P_{O_2}$ , and the plot of  $\ln(P_{O_2})$  versus  $1/T$  is linear, as expected for a system at equilibrium. However, the apparent equilibrium  $O_2$  pressures are much higher than expected from thermodynamic analysis.<sup>5</sup> Despite the reversible steady state observed, we show that the alumina structures are not in global equilibrium with gaseous  $O_2$  and NiAl. We discuss the possible origins of this kinetic steady state.

### II. EXPERIMENTAL DETAILS

Our low-energy electron microscopy<sup>12</sup> (LEEM) experiments were conducted in a vacuum system with a base pressure below  $1 \times 10^{-10}$  Torr. The substrate temperature was measured by a W-5%Re/W-26%Re thermocouple spot welded to the side of our disk-shaped crystal.  $O_2$  pressure was measured by an ionization gauge. The NiAl(110) surface was prepared with several cycles of sputtering with 1500 eV Ar ions and anneals to 1250 K. We quantified the stability of alumina islands on NiAl(110) by using the following procedure. The crystal was held at 800–1350 K and the  $O_2$  pressure in the chamber was increased until alumina islands and/or oxide rods were observed to nucleate on the clean substrate. The  $O_2$  pressure was then reduced and held constant. If the small structures in the field of view grew, the pressure was further reduced. If the structures shrunk, the  $O_2$

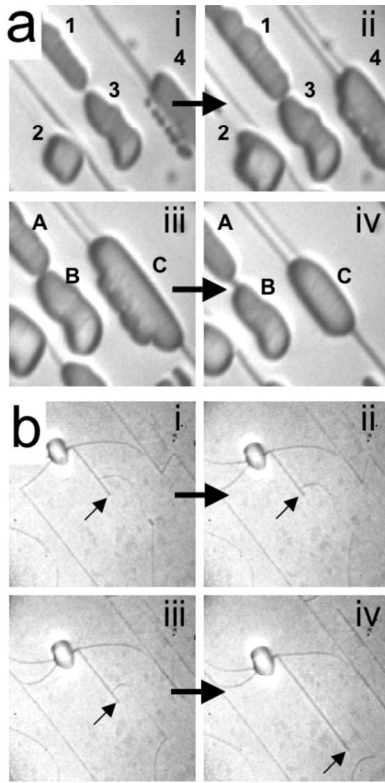


FIG. 1. LEEM images of oxide structures in  $O_2$  atmospheres greater and less than needed for apparent equilibrium. (a) At 1268 K, the alumina islands grow (i-ii) in  $3.67 \times 10^{-7}$  Torr  $O_2$  and shrink (iii-iv) in  $5.65 \times 10^{-8}$  Torr  $O_2$ . Corresponding islands are labeled in consecutive images. (b) At 1083 K, the free end of the rod (arrow) retracts (i-ii) when  $P_{O_2} = 1.15 \times 10^{-9}$  Torr and advances (iii-iv) when  $P_{O_2} = 5.6 \times 10^{-9}$  Torr. Images are  $3 \times 3 \mu m^2$ .

pressure was increased. Total  $O_2$  doses were 3–20 L ( $1 L = 10^{-6}$  Torr s).

Wavelength-dispersive electron microprobe analysis showed that our crystal is Ni rich, with a composition near  $Ni_{0.57}Al_{0.43}$ . Whether the rods formed depended on the substrate's composition. After enriching the near-surface region by depositing several monolayers of Al,<sup>13</sup> only alumina islands formed. If the NiAl crystal was annealed at high temperature for extended periods, rods again formed on the surface, presumably because annealing depletes the near-surface region in Al (either through bulk diffusion or preferential evaporation of Al).

### III. RESULTS

#### A. Oxygen pressures needed to stabilize alumina films

To probe the stability of the surface oxides, we observe whether individual aluminum-oxide structures grow or shrink as a function of  $O_2$  pressure and substrate temperature. Figure 1 shows an example of how both types of oxides respond to changing  $O_2$  pressure, as observed in real time by using LEEM. Images (i) and (ii) of Fig. 1(a) show that the alumina islands grow at the given  $O_2$  pressure. Decreasing the pressure, however, causes the islands to shrink [images

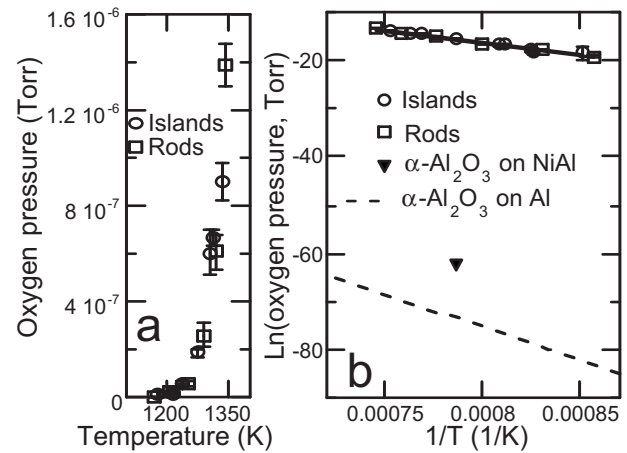


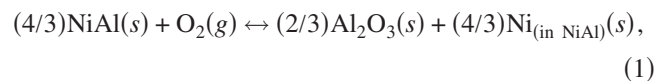
FIG. 2. (a) Temperature dependence of  $O_2$  pressure at apparent equilibrium for oxide islands and rods. The steady-state pressure is the average of the highest (error bar bottom) and lowest (error bar top) pressures at which the structures were observed to decompose and grow, respectively. (b)  $\ln(P_{O_2})$  vs  $1/T$  measured and calculated if  $\alpha-Al_2O_3$  is in equilibrium with NiAl at 1273 K (see Appendix A) or Al [from  $\Delta G^0 = -11.67 + 0.002272T$  eV/ $O_2$  molecule (Ref. 29) and Eq. (2)].

(iii) and (iv)]. The rods exhibit a similar behavior [Fig. 1(b)]. These observations show that a dynamic steady state exists between the alumina structures and the gaseous  $O_2$ .

The pressure at which the nanostructures neither grew nor shrunk at a fixed temperature,  $P_{O_2}$ , could be bracketed within a small range of values [see Fig. 2(a)]. Within experimental uncertainty, the two oxide phases are identically stable despite having different epitaxial relationships with the substrate and markedly different morphologies. At 1273 K, for example, both types of oxides are apparently in equilibrium in an atmosphere of  $2.0 \times 10^{-7}$  Torr  $O_2$ . At the same temperature, the  $O_2$  partial pressure in equilibrium with NiAl and bulk  $\alpha-Al_2O_3$  is  $9.0 \times 10^{-28}$  Torr [see Fig. 2(b) and Appendix A], as calculated from the tabulated free energies of  $O_2$ , NiAl, and  $\alpha-Al_2O_3$ . Thus, the surface oxide phases appear to be much less stable than bulk alumina. However, first-principles calculations suggest that the formation energy (and, thus, the equilibrium  $O_2$  pressure) of the surface oxide is close to that of bulk  $\alpha-Al_2O_3$  (see below).<sup>6,14</sup> If we assume that our experimental system is in equilibrium, the factor of  $10^{20}$  discrepancy in  $O_2$  pressures is quite puzzling.

#### B. Thermodynamic analysis shows that the system is not in equilibrium

Next we examine the discrepancy's origins by using the experimental data to calculate the Gibbs formation energy of the two surface alumina types, islands and rods, assuming that they are in global equilibrium with gaseous  $O_2$  and NiAl. With the Al at its chemical potential in NiAl alloy and if both alumina types are, for simplicity, assumed to have stoichiometry  $Al_2O_3$ , we have



in which the unoxidized Ni is absorbed into bulk NiAl.<sup>5</sup> Then the reaction's standard Gibbs free energy  $\Delta G^0(T)$ ,

which is the free energy change at  $P_{O_2}=1$  atm, in terms of the rate constant  $K$ , is

$$\Delta G^0(T) = -RT \ln(K) = -RT \ln\left(\frac{1}{P_{O_2}^{eq}}\right) = RT \ln(P_{O_2}^{eq}), \quad (2)$$

in which  $R$  is the gas constant,  $T$  is the temperature in degrees Kelvin, and  $P_{O_2}^{eq}$  is the pressure at which the condensed phases are at equilibrium with the  $O_2$  gas.<sup>15</sup> Since  $\Delta G^0 = \Delta H^0 - T\Delta S^0$ ,

$$\ln P_{O_2}^{eq} = \frac{\Delta H^0}{R} \left(\frac{1}{T}\right) - \frac{\Delta S^0}{R}, \quad (3)$$

for  $P$  in units of atm. We initially assume that  $P_{O_2}^{eq}$  is the pressure at which the alumina structures neither grow nor shrink [Fig. 2(a)].

Figure 2(b) shows that the plots of  $\ln(P_{O_2}^{eq})$  versus  $1/T$  are linear for both the alumina islands and rods. Thus, the temperature dependence of the  $O_2$  pressures exhibits the behavior anticipated for an equilibrium reaction with gaseous  $O_2$ , such as Eq. (1). Values for  $\Delta H^0$  (the standard enthalpy change) and  $\Delta S^0$  (the standard entropy change) are determined, respectively, from the slope and intercept. Then  $\Delta G^0(T)$  for the alumina islands and rods are

$$\Delta G_{islands}^0 = (-4.57 \pm 0.30) - (-0.00168 \pm 0.000245)T \quad (4a)$$

and

$$\Delta G_{rods}^0 = (-4.35 \pm 0.18) - (-0.00150 \pm 0.000290)T, \quad (4b)$$

in units of eV/ $O_2$  molecule. At 1273 K,  $\Delta G_{islands}^0 = -2.43 \pm 0.43$  eV/ $O_2$  molecule and  $\Delta G_{rods}^0 = -2.44 \pm 0.41$  eV/ $O_2$  molecule. At the same temperature, in contrast, the formation energy of bulk  $\alpha-Al_2O_3$  is  $\Delta G^0 = -7.56$  eV/ $O_2$  molecule.<sup>16</sup> That is, if our measured steady-state  $O_2$  pressures are interpreted as the equilibrium pressures as in Eq. (1), the alumina structures are about 5.1 eV/ $O_2$  less stable than bulk  $\alpha-Al_2O_3$ .

This huge energy difference between the known free energy of bulk  $\alpha-Al_2O_3$  and that calculated for the alumina islands and rods from the measured  $O_2$  pressure at steady state is hard to reconcile with the lack of bulk  $\alpha-Al_2O_3$  formation. That is, if the aluminum-oxide structures on NiAl were, indeed, about 5 eV/ $O_2$  less stable than the bulk oxide, they should never form. Indeed, NiAl forms bulk oxides in closed environments at extremely low  $O_2$  pressures, as low as  $10^{-19}$  Torr at about 800 °C.<sup>17</sup> The incorrect assumption of Eq. (1) is that gaseous  $O_2$  is in equilibrium with the alumina islands and NiAl. This point is reinforced by state-of-the-art calculations of the complex  $Al_{10}O_{13}$  structure on NiAl(110).<sup>14</sup> These calculations show a formation energy (about -9 eV/ $O_2$  at  $T=0$  K and assuming that the Al chemical potential in NiAl is 1 eV below that for fcc-Al) close to bulk alumina but much larger than our equilibrium analysis [Eqs. (4a) and (4b)].

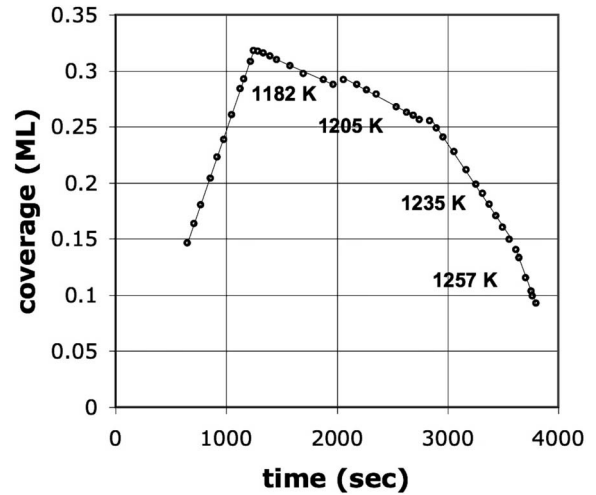


FIG. 3. Coverage of alumina islands versus time during oxidation with  $7.9 \times 10^{-8}$  Torr  $O_2$  with the substrate at 1182 K, and during reduction (loss) by vacuum annealing at various temperatures. During  $O_2$  exposure, the fractional coverage of oxide linearly increased in time. At 1200 s,  $O_2$  was evacuated and the alumina began to decompose.

### C. Bounding the effect of gas temperature

Before we discuss the possible origins of why the alumina films have large  $O_2$  vapor pressures, we must reject one possible cause. Our experiment differs from the ideal situation where the  $O_2$  gas and NiAl temperature are the same. Instead, the gas is at room temperature. If there was a substantial barrier to  $O_2$  dissociation on the surface,<sup>18</sup> only a fraction of  $O_2$  molecules proportional to those having a kinetic energy greater than the barrier would dissociate. Our attempts to directly investigate the effect of gas temperature on the steady-state pressure by using hot  $O_2$  molecules produced from a line-of-sight, high-temperature effusion cell failed because most  $O_2$  molecules striking the surface were still the ones that had equilibrated by previous collisions with the room-temperature chamber walls.

We are able, however, to calculate an upper bound on the effect of gas temperature by measuring the rate at which alumina grows and by knowing the rate of  $O_2$  impingement. The probability  $P_{att}$  that an  $O_2$  molecule that strikes the surface becomes incorporated into alumina islands is  $P_{att} = R_{att}/R_{imp}$ , where  $R_{att}$  is the rate at which  $O_2$  attaches to the alumina and  $R_{imp}$  is the  $O_2$  impingement rate. At steady state, the rate at which oxygen attaches to an alumina island is equal to the detachment rate:  $R_{att} = R_{det}$ . We measure  $R_{det}$  directly from the rate at which the alumina islands shrink when heated in vacuum (see Fig. 3).  $R_{imp}$  is calculated from  $P_{O_2}$ , which is the measured  $O_2$  pressure at apparent equilibrium [Fig. 2(a)] as follows:

$$R_{imp} = \frac{P_{O_2} N_A}{\sqrt{2\pi MRT}},$$

where  $N_A$  is Avogadro's number,  $M=0.032$  kg/mole,  $R=8.314$  J/(mol K), and  $T=298$  K. Since the alumina islands contain  $2.56 \times 10^{15}$  atoms/(cm<sup>2</sup> double layer),<sup>19</sup>

TABLE I. Fraction of  $O_2$  molecules that react to form an oxide ( $P_{att}$ ) at steady state, as determined from desorption rates from Fig. 3 and impingement rates derived from the steady-state pressures  $P_{O_2}^{eq}$  in Fig. 2(a).

$T$ (K)	Desorption rate (ML/s)	Impingement rate (ML/s)	$P_{att}$
1205	$5.3 \times 10^{-5}$	$5.6 \times 10^{-3}$	1/106
1235	$1.5 \times 10^{-4}$	$1.5 \times 10^{-2}$	1/100
1257	$2.7 \times 10^{-4}$	$2.8 \times 10^{-2}$	1/104

$R_{imp} = 2.810 \times 10^5 P_{O_2}$  in units of alumina double layers/s, with  $P_{O_2}$  in Torr. For substrate temperatures at around 1200 K (see Table I), we find  $P_{att} \approx 0.01$  for 298 K  $O_2$ .

To place an upper bound on the effect of gas temperature, consider the most extreme case—that *every* impinging  $O_2$  incorporates into the alumina film when the gas and substrate temperatures are equal. Then  $\sim 100$  times fewer impinging  $O_2$  molecules would be needed to maintain a steady state with  $\sim 1200$  K gas than with a 298 K gas. However, the actual pressure of the 1273 K gas, for example, needed for this lower impingement rate is  $(298/1273)^{0.5} = 0.48$  times the pressure of the 298 K gas. Thus, the steady-state pressure of 1273 K  $O_2$  can be at most  $\sim 100 \times 0.48 \approx 48$  times less than the 298 K value. Since the  $O_2$  pressures needed to stabilize ultrathin alumina (Fig. 2) and those predicted from bulk  $\alpha$ - $Al_2O_3$  thermodynamic data differ by 20 orders of magnitude, we are confident that gas temperature contributes only negligibly to this difference.

#### IV. DISCUSSION

##### A. Origins of high oxygen vapor pressure needed to stabilize films

So why is the  $O_2$  pressure needed to stabilize alumina films on NiAl so remarkably high? Before discussing likely explanations, we first consider the microscopic mechanisms by which oxidation or reduction occurs. Our LEEM observations are consistent with the oxidation and reduction of NiAl occurring by a mechanism involving the diffusion of surface species, such as adatoms or clusters, similar to the oxidation of some metals such as Ni.<sup>20</sup> That is, alumina growth and loss behave like typical film growth and evaporation. Specifically, we find that the nucleation behavior is quantitatively described by traditional theories of surface nucleation.<sup>21</sup> For example, we find that the areal density of the oxide nuclei saturates with time and that the density of nuclei decreases with increasing substrate temperature. We also find that the growth rate of alumina islands depends on their local environment (i.e., proximity to neighboring islands). This observation is consistent with the growth species being partitioned by surface diffusion among the various islands.

The schematic in Fig. 4(a) then represents the simplest reaction model consistent with the LEEM observations: surface diffusion of oxide precursors, exchange of Al surface species with the NiAl bulk, and exchange of O surface spe-

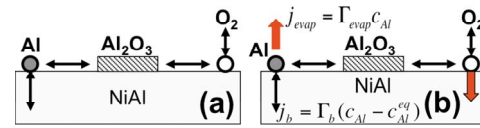


FIG. 4. (Color online) (a) Schematic of equilibrium between an alumina film,  $O_2$  vapor, and Al atoms in NiAl. (b) Possible (non-equilibrium) steady state, showing fluxes of Al atoms into the vapor (left) or oxygen atoms (right) into the substrate. Because of these fluxes, the  $O_2$  pressure needed to establish a steady state can be dramatically higher than the equilibrium pressure.

cies with the  $O_2$  gas. This model in global equilibrium leads to Eq. (1). However, the quantitative analysis given above shows that this model cannot be correct.

Given that diffusing surface species are responsible for the growth and reduction of the surface oxides, we suggest two processes that could lead to the much-higher-than-anticipated O vapor pressures—Al may be desorbing from the surface or oxygen may be diffusing into the NiAl bulk.<sup>22</sup> These scenarios are illustrated in Fig. 4(b). (We note that other scenarios that lead to the nonequilibrium steady state are also possible. For example, species like  $AlO_x$  that are not supplied from the gas phase may be evaporating from the surface. In fact, the size of the discrepancy may be a hint that more than one surface species is out of equilibrium.) Given its thickness, the crystal is essentially an infinite sink for O or a source of Al over the time scale of our experiments. Regarding Al evaporation, literature suggests that the vapor pressure of Al over NiAl is significant at the temperatures of our experiment, for example,  $4 \times 10^{-8}$  Torr for our crystal composition ( $Ni_{57}Al_{43}$ ) at 1273 K.<sup>23</sup> Thus, the Al surface concentration may become depressed at elevated temperature. Whether or not O is significantly soluble in NiAl is an open question in literature—some works have argued against<sup>24</sup> subsurface O diffusion, but more recent work provides evidence of some bulk solubility.<sup>25</sup> We see no direct evidence of this behavior, but we certainly cannot exclude it because O diffusion into the bulk may be fast at the relatively high temperatures of our experiments.

##### B. Kinetic steady states far from equilibrium

The analysis in Sec. III B shows that some processes in the  $O_2$ /alumina/NiAl system must be far from equilibrium. For concreteness, we next show an example of how a steady-state balance between two kinetic processes can greatly alter a system's apparent stability relative to that of global equilibrium. That is, we consider the case of two processes that are dynamically balanced (in "local" equilibrium) but which are not in equilibrium with other reactions. We consider the scenario of Al evaporation from the surface being the dominant nonequilibrium process, but emphasize that a similar conclusion is reached for the scenario of O dissolving into the NiAl. Given an Al adatom density on the surface,  $c_{Al}$ , the Al chemical potential  $\mu_{Al}$  differs from its equilibrium value by

$$\Delta\mu_{Al} \approx k_B T \ln c_{Al} - k_B T \ln c_{Al}^{eq} = k_B T \ln(c_{Al}/c_{Al}^{eq}),$$

where  $c_{Al}^{eq}$  is the true equilibrium concentration and  $k_B$  is the Boltzmann constant. Then consider when  $c_{Al}$  is determined

by the condition that the Al flux from the NiAl bulk to the surface,  $j_b = \Gamma_b(c_{\text{Al}} - c_{\text{Al}}^{\text{eq}})$ , is in steady state with the evaporation flux,  $j_{\text{evap}} = \Gamma_{\text{evap}}c_{\text{Al}}$ , where  $\Gamma_b$  and  $\Gamma_{\text{evap}}$  are the rate constants of bulk/surface exchange and evaporation, respectively. Taking  $j_b + j_{\text{evap}} = 0$  gives  $c_{\text{Al}} = \Gamma_b c_{\text{Al}}^{\text{eq}} / (\Gamma_b + \Gamma_{\text{evap}}) < c_{\text{Al}}^{\text{eq}}$ . Then  $\Delta\mu_{\text{Al}} = k_B T \ln[\Gamma_b / (\Gamma_b + \Gamma_{\text{evap}})]$ , which can be large if  $\Gamma_b \ll \Gamma_{\text{evap}}$ , that is, if supplying Al from the bulk is slow compared to Al evaporation. Thus, as the evaporation rate increases, the Al surface concentration can become increasingly smaller than the true equilibrium value. However, can this scenario account for the 20 orders of magnitude discrepancy we observe? In fact, given that bulk diffusion of Ni and Al in NiAl is relatively fast,<sup>26</sup> it is unlikely that the bulk is depleted in Al just below the surface. However, we next argue that surface adspecies concentration can be considerably lower than might be predicted from bulk properties because the creation of adspecies can be relatively slow.

The creation of surface thermal defects can be slow compared to bulk diffusion. For example, the creation of an adatom on a terrace requires the generation of an energetically costly adatom—vacancy pair. Consistent with this, our previous work only observed mass exchange between the NiAl surface and bulk at the surface steps, not over the entire terrace.<sup>27,28</sup> In Appendix B, we give simple arguments that show how the inability of the terraces to exchange mass can greatly reduce the Al adatom concentration. Two limiting cases are considered, where the rate of Al adatom generation at the steps is either fast or slow compared to the rate at which Al diffuses away from the steps and evaporates. When Al adatom generation at steps is relatively fast, the Al concentration exponentially decreases with distance from the steps. If the surface diffusion constant is small compared to the evaporation rate, undersaturations can be very large. In the other limit, when diffusion is fast, the rate of Al evaporation is limited by the rate at which Al adatoms are generated at steps. This makes  $\Gamma_b$  proportional to step density. On substrates such as ours, with steps roughly every micron, the supply of Al from the bulk is very roughly  $10^{-4}$  less than if Al adatoms were uniformly created on the surface. In either limit, the Al adatom concentration can be orders of magnitude lower than anticipated because adatoms are only created at steps.

Again, we know that the  $\text{O}_2$ /alumina/NiAl system exists in some kinetic steady state far from true equilibrium. Given fast bulk diffusion,<sup>26</sup> we suggest that the concentration of one or more surface species, such as Al in the unproven scenario just discussed, must be far below its equilibrium value. In a chemical reaction such as Eq. (1), the law of mass action dictates that if one reactant's concentration (Al, in the above scenario) is reduced, the other reactant's concentration (O) must be increased to maintain local equilibrium between the reactants. Indeed, our observations suggest that the alumina film is in local equilibrium with the concentration of Al and O species at the surface—above and below our measured steady-state  $\text{O}_2$  pressure, islands grow and shrink, respectively. What is out of equilibrium is either the surface concentrations of Al (no Al is supplied from the gas phase in the experiment) or oxygen (oxygen may be diffusing into the bulk).

## V. SUMMARY

The alumina islands clearly wet the NiAl(110) substrate—once nucleated, the islands grow until they cover the substrate (see Fig. 3). Thermodynamic analysis<sup>2</sup> then predicts that the surface alumina should be more stable than bulk alumina. Yet the  $\text{O}_2$  pressure required to stabilize the oxide films is vastly higher than that of bulk alumina. Applying thermodynamics to the nonequilibrium system of surface oxides on NiAl is clearly not appropriate. Our results do highlight how far from equilibrium a system can be maintained in a kinetic steady state. The substantial deviations from equilibrium behavior of other film/substrate systems<sup>5</sup> may also arise from kinetic effects like those described here.

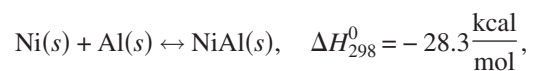
We also point out that monitoring how individual small structures of known phase and size respond to environmental changes is a useful approach to access whether a system is unstable (evolving), at local equilibrium, or in global equilibrium. An imaging technique complements other techniques (surface x-ray diffraction,<sup>13</sup> thermal desorption,<sup>14</sup> and precise mass measurements<sup>15</sup>) that monitor film stability averaged over large surface areas. In systems that are in equilibrium, an imaging approach can determine, for example, how the Gibbs formation energy depends on size and structure. Even for systems at steady state, such as alumina on NiAl, the method can still accurately access the relative stability of different phases and structure sizes.

## ACKNOWLEDGMENT

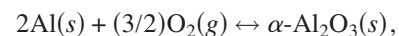
This work was supported by the Office of Basic Energy Sciences, Division of Materials Sciences of the U.S. Department of Energy under Contract No. DE-AC04-94AL85000.

## APPENDIX A: EQUILIBRIUM THERMODYNAMICS

In this appendix, we document the thermodynamic values used to calculate the oxygen partial pressure that would be in equilibrium with bulk  $\alpha\text{-Al}_2\text{O}_3$  and the Al in NiAl. We calculate the standard Gibbs free energy  $\Delta G^0(T)$  of the reaction given in Eq. (1) by using the following experimental data from Kubaschewski and Alcock:<sup>16</sup>



$$S_{298}^0 = 12.93 \frac{\text{cal}}{\text{mol K}},$$



$$\Delta H_{298}^0 = -400.9 \frac{\text{kcal}}{\text{mol}}, \quad S_{298}^0 = 12.2 \frac{\text{cal}}{\text{mol K}},$$

$$\text{Ni}: \quad \Delta H_{298}^0 = 0, \quad S_{298}^0 = 7.14 \frac{\text{cal}}{\text{mol K}},$$

$$\text{O}_2: \quad \Delta H_{298}^0 = 0, \quad S_{298}^0 = 49.0 \frac{\text{cal}}{\text{mol K}},$$

and the experimental value from Lozovoi *et al.*:<sup>29</sup>  
 $\text{Ni}(s) \leftrightarrow \text{Ni}(\text{in Ni}_{0.55}\text{Al}_{0.45})(s),$

$$\Delta G_{1273}^0 = -4.86 \frac{\text{kcal}}{\text{mol}}.$$

We account for the temperature dependence by using the approximate relationship<sup>16</sup>

$$\Delta G^0(T) = \Delta T_{298}^0 - T \Delta S_{298}^0.$$

For reaction 1 at 1273 K, we then have  $\Delta G_{1273}^0 = -7.56 \text{ eV/O}_2 = kT \ln(P_{\text{O}_2}^{eq}/760)$  and  $P_{\text{O}_2}^{eq} = 9 \times 10^{-28} \text{ Torr}$ , which are in good agreement with the results of Finnis *et al.*<sup>5</sup> We note that the alloy composition only has a small effect on  $P_{\text{O}_2}^{eq}$  (see Fig. 3 of Ref. 5).

## APPENDIX B: ADATOM CONCENTRATIONS

Here, we examine how the concentration of a surface adspecies behaves if the adspecies are only created at substrate steps but evaporate from the entire surface. We consider two limiting cases. First, no substantial energy barrier exists for creating the adspecies at the step, so the rate of adspecies loss is determined by the surface diffusion and evaporation rates. Second, an energy barrier exists to adspecies creation at substrate steps, which makes equilibration on the surface slow. For the first case, consider how the adatom concentration, Al, for example, evolves near a substrate step. We assume the flux from the bulk to the step to be

$$j_{\text{step}} = \Gamma_{\text{step}} [c_{\text{Al}}^{eq} - c_{\text{Al}}(0)],$$

where  $\Gamma_{\text{step}}$  gives the rate of bulk/surface mass exchange at the substrate step. In steady state, this flux is balanced by a flow onto the terrace,  $j_{\text{terrace}}$ , where evaporation occurs. The diffusion equation for the steady-state concentration profile that determines this flux is

$$\frac{\partial c_{\text{Al}}}{\partial t} = D \nabla^2 c_{\text{Al}} - \Gamma_{\text{evap}} c_{\text{Al}} = 0,$$

where  $D$  is the surface diffusion constant. The solution is

$$c_{\text{Al}}(x) = c_{\text{Al}}(0) \exp\left(-\sqrt{\frac{\Gamma_{\text{evap}}}{D}} x\right),$$

where  $x$  is the direction perpendicular to the step. Setting  $j_{\text{step}} = j_{\text{terrace}}$  gives

$$\Gamma_{\text{step}} [c_{\text{Al}}^{eq} - c_{\text{Al}}(0)] = -D \nabla c_{\text{Al}}|_{x=0} = c_{\text{Al}}(0) \sqrt{\Gamma_{\text{evap}} D}.$$

Then the Al surface concentration at the step  $c_{\text{Al}}(0)$  is

$$\frac{c_{\text{Al}}^{eq} - c_{\text{Al}}(0)}{c_{\text{Al}}(0)} = \frac{\sqrt{\Gamma_{\text{evap}} D}}{\Gamma_{\text{step}}}.$$

In the limit  $\sqrt{\Gamma_{\text{evap}} D} / \Gamma_{\text{step}} \gg 1$ , we have

$$c_{\text{Al}}(0) = c_{\text{Al}}^{eq} \frac{\sqrt{\Gamma_{\text{evap}} D}}{\Gamma_{\text{step}}}$$

and

$$c_{\text{Al}}(x) = \frac{c_{\text{Al}}^{eq} \Gamma_{\text{step}}}{\sqrt{\Gamma_{\text{evap}} D}} \exp\left(-\sqrt{\frac{\Gamma_{\text{evap}}}{D}} x\right).$$

Thus, the Al concentration on the terrace is exponentially lower than next to the step, which leads to potentially large adatom undersaturations if  $D$  is small compared to  $\Gamma_{\text{evap}}$ .

For a large step detachment barrier, which is the second limiting case, the rate of change of adspecies concentration is proportional to the ratio of step length  $l$  to terrace area  $A$  as follows:

$$\frac{\partial c_{\text{Al}}}{\partial t} = \Gamma_{\text{step}} (c_{\text{Al}} - c_{\text{Al}}^{eq}) \frac{l}{A}.$$

Then  $\Gamma_b$  in Sec. IV B is proportional to  $l/A \approx 10^{-4}$  for terraces  $1 \mu\text{m}$  wide, with  $\Gamma_{\text{step}}$  in units of lattice spacing, again leading to large potential undersaturations.

\*piercejp@gmail.com

<sup>1</sup>L. B. Freund and S. Suresh, *Thin Film Materials* (Cambridge University Press, Cambridge, England, 2003), p. 550.

<sup>2</sup>C. T. Campbell, *Phys. Rev. Lett.* **96**, 066106 (2006).

<sup>3</sup>K. Reuter and M. Scheffler, *Phys. Rev. Lett.* **90**, 046103 (2003).

<sup>4</sup>W. Zhang, J. R. Smith, and X. G. Wang, *Phys. Rev. B* **70**, 024103 (2004).

<sup>5</sup>M. W. Finnis, A. Y. Lozovoi, and A. Alavi, *Annu. Rev. Mater. Res.* **35**, 167 (2005).

<sup>6</sup>G. Kresse, M. Schmid, E. Napetschnig, M. Shishkin, L. Kohler, and P. Varga, *Science* **308**, 1440 (2005).

<sup>7</sup>E. Lundgren, J. Gustafson, A. Mikkelsen, J. N. Andersen, A. Stierle, H. Dosch, M. Todorova, J. Rogal, K. Reuter, and M. Scheffler, *Phys. Rev. Lett.* **92**, 046101 (2004).

<sup>8</sup>H. Gabasch, W. Unterberger, K. Hayek, B. Klotzer, G. Kresse, C. Klein, M. Schmid, and P. Varga, *Surf. Sci.* **600**, 205 (2006).

<sup>9</sup>R. M. Jaeger, H. Kuhlenbeck, H. J. Freund, M. Wuttig, W. Hoffmann, R. Franchy, and H. Ibach, *Surf. Sci.* **259**, 235 (1991).

<sup>10</sup>J. P. Pierce and K. F. McCarty, *Phys. Rev. B* **71**, 125428 (2005).

<sup>11</sup>K. F. McCarty, J. P. Pierce, and C. B. Carter, *Appl. Phys. Lett.* **88**, 141902 (2006).

<sup>12</sup>E. Bauer, *Rep. Prog. Phys.* **57**, 895 (1994).

<sup>13</sup>J. P. Pierce, N. C. Bartelt, and K. F. McCarty, *Phys. Rev. Lett.* **99**, 026101 (2007).

<sup>14</sup>G. Kresse (private communication).

<sup>15</sup>D. R. Gaskell, *Introduction to Metallurgical Thermodynamics* (McGraw-Hill, New York, 1973), p. 244.

<sup>16</sup>O. Kubaschewski and C. B. Alcock, *Metallurgical Thermochemistry*, 5th ed. (Pergamon, Oxford, 1979), pp. 19 and 268.

<sup>17</sup>M. W. Brumm, H. J. Grabke, and B. Wagemann, *Corros. Sci.* **36**, 37 (1994).

<sup>18</sup>K. W. Kolasinski, *Surface Science* (Wiley, West Sussex, 2002),

- p. 107.
- <sup>19</sup>J. Libuda, F. Winkelmann, M. Baumer, H. J. Freund, T. Bertrams, H. Neddermeyer, and K. Muller, *Surf. Sci.* **318**, 61 (1994).
- <sup>20</sup>P. H. Holloway and J. B. Hudson, *Surf. Sci.* **43**, 123 (1974).
- <sup>21</sup>J. A. Venables, G. D. T. Spiller, and M. Hanbucken, *Rep. Prog. Phys.* **47**, 399 (1984).
- <sup>22</sup>F. Qin, J. W. Andereg, C. J. Jenks, B. Gleeson, D. J. Sordelet, and P. A. Thiel, *Surf. Sci.* **601**, 146 (2007).
- <sup>23</sup>D. Raj, L. Bencze, D. Kath, W. A. Oates, J. Herrmann, L. Singheiser, and K. Hilpert, *Intermetallics* **11**, 1119 (2003).
- <sup>24</sup>A. Katsman, H. J. Grabke, and L. Levin, *Oxid. Met.* **46**, 313 (1996).
- <sup>25</sup>E. Loginova, F. Cosandey, and T. E. Madey, *Surf. Sci.* **601**, L11 (2007).
- <sup>26</sup>H. Wei, X. F. Sun, Q. Zheng, H. R. Guan, and Z. Q. Hu, *Acta Mater.* **52**, 2645 (2004).
- <sup>27</sup>K. F. McCarty, J. A. Nobel, and N. C. Bartelt, *Nature (London)* **412**, 622 (2001).
- <sup>28</sup>K. F. McCarty, J. A. Nobel, and N. C. Bartelt, *Phys. Rev. B* **71**, 085421 (2005).
- <sup>29</sup>A. T. Lozovoi, A. Alavi, and M. W. Finnis, *Comput. Phys. Commun.* **137**, 174 (2001).